SLAC-PUB-6002
NOVEMBER 1992
(E)

Measurement of the Tau Lepton Mass by the Beijing Spectrometer (BES) Collaboration*

E. Soderstrom
Stanford Linear Accelerator Center
Stanford University, Stanford, CA 94309
Representing the BES Collaboration[1]

ABSTRACT

The mass of the τ lepton has been measured at the Beijing Electron Positron Collider using the Beijing Spectrometer. A search near threshold for $e^+e^- \to \tau^+\tau^-$ was performed. Candidate events were identified by requiring that one τ decay via $\tau \to e\nu\bar{\nu}$, and the other via $\tau \to \mu\nu\bar{\nu}$. The mass value, obtained from a fit to the energy dependence of the $\tau^+\tau^-$ cross section, is $m_\tau = 1776.9^{+0.4}_{-0.5} \pm 0.2$ MeV.

1 INTRODUCTION

It has recently been the focus of much attention that the current[2] (RPP92) averages of the tau electronic branching ratio $B^e_\tau = (17.93 \pm 0.26)\%$, lifetime $t_\tau = (3.05 \pm 0.06) \times 10^{-13}$ s, and mass $m_\tau = 1784.1^{+2.7}_{-3.6}$ MeV are inconsistent at the 2.4 σ level with the lepton universality implied by the SU(2)×U(1) gauge symmetry of the Standard Model. Within this model leptonic decay rates are given by[3]

$$\Gamma(L \to \nu_L l \nu_l(\gamma)) = \frac{G_L^2 m_L^5}{192\pi^3} \times F_{cor}(m_L, m_l), \tag{1}$$

where m_L is the mass of the parent lepton L, G_L is the Fermi weak coupling constant and the correction factor Π F_{cor} is given by

$$F_{cor} = f(\frac{m_l^2}{m_L^2}) \times F_W \times F_{RAD}, \tag{2}$$

with

$$f(x) = 1 - 8x + 8x^3 - x^4 - 12x^2 \ln x, \tag{3}$$

*Work supported by the Department of Energy, contract DE-AC03-76SF00515.

Presented at the 20th Annual SLAC Summer Institute on Particle Physics Topical Conference, Stanford, CA, July 13 - 24, 1992.

$$F_W = \left[1 + \frac{3}{5}\frac{m_L^2}{m_W^2}\right] , \tag{4}$$

and

$$F_{RAD} = \left[1 + \frac{\alpha(m_L)}{2\pi}(\frac{25}{4} - \pi^2)\right] . \tag{5}$$

The function $f(x)$ comes directly out of the matrix element for τ decay integrated over the standard three body final state phase space. The correction factor F_W accounts for the non-local structure of the W-propagator, and the factor F_{RAD} arises due to initial and final state radiative corrections. It should be noted that substituting the RPP92 values $m_\mu = 105.658389 \pm 0.000034$MeV, $t_\mu = (2.19703 \pm 0.00004) \times 10^{-6}$ s, $M_W = 80.22 \pm 0.26$ GeV and also[3] $\alpha(m_\mu)^{-1} = 136$ into Equation (1) yields the current value for the Fermi weak coupling constant $G_F = 1.16639 \times 10^{-5}\text{GeV}^{-2}$.

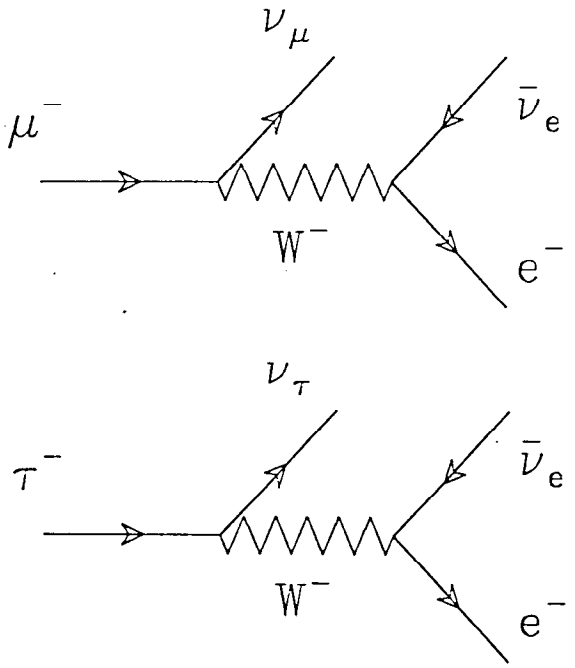

Figure 1: Lowest order diagrams for the electronic decays of the muon and tau lepton.

The electronic decays of the τ and muon shown in Figure 1 can be related through Equation (1); the substitutions $\Gamma(\tau \to \nu_\tau e \nu_e) = B_\tau^e/t_\tau$ and $\Gamma(\mu \to \nu_\mu e \nu_e) = 1/t_\mu$ yield

$$\left(\frac{G_{\tau\to e\nu\bar{\nu}}}{G_{\mu\to e\nu\bar{\nu}}}\right)^2 = \left(\frac{m_\mu}{m_\tau}\right)^5 \left(\frac{t_\mu}{t_\tau}\right) B_\tau^e, \tag{6}$$

Table 1: Corrections given by Equations (3)-(5), calculated for the decays of the muon and tau, with $\alpha(m_\mu)^{-1} = 136$ and $\alpha(m_\tau)^{-1} = 131$.[3]

Correction	Value
$f(m_e^2/m_{\mu^2})$	0.9998
$F_W(m_\mu)$	1.0000
$F_{RAD}(m_\mu)$	0.9956
$f(m_e^2/m_{\tau^2})$	1.0000
$F_W(m_\tau)$	1.0003
$F_{RAD}(m_\tau)$	0.9957

where the corrections for the muon and tau listed in Table 1 together contribute to the ratio of the coupling constants at the level of 4 parts in 10^4 and are thus neglected. Inserting the RPP92 values for the masses, lifetimes and branching fraction into Equation (6) gives

$$\left(\frac{G_{\tau\to e\nu\bar{\nu}}}{G_{\mu\to e\nu\bar{\nu}}}\right)^2 = 0.941 \pm 0.025 \tag{7}$$

and the 2.4 σ inconsistency with the unity ratio implied by lepton universality is obtained. This so called "Consistency Problem" is illustrated in Fig 2.

It is entirely possible that the above inconsistency is due to measurement error or bias in one or more of the tau lifetime, branching fraction or mass parameters. The measurements which result in the RPP92 average values of these quantities are shown in Figures 3 - 5.

It is clear from Figure 5 that the value of the tau mass is dominated by the DELCO result[4] $m_\tau = 1783^{+3}_{-4}$ MeV. In that experiment, $\tau^+\tau^-$ events were identified by selecting non-collinear 2-prong events with one track identified as an electron(positron) and the other, X, identified as **non**-positron(electron) to measure the cross section ratio

$$R = \frac{\sigma(e^+e^- \to e + X + \ldots)}{\sigma(e^+e^- \to \mu^+\mu^-)}, \quad X \neq \bar{e} \tag{8}$$

over a broad center-of-mass energy range, $3.1 \leq W \leq 7.4$ GeV. The ratio R provides a measure of the energy dependence of the cross section for $e^+e^- \to \tau^+\tau^-$ from threshold up to 7.4 GeV, and a fit to this dependence yields an estimate of the threshold energy, and hence of the tau mass. This procedure led to a few MeV uncertainty in the value of m_τ. To improve on this, BES uses only non-collinear 2-prong $e\mu$ final states where the e and μ are well-identified; this provides a virtually background free event sample corresponding to the $\tau^+\tau^-$

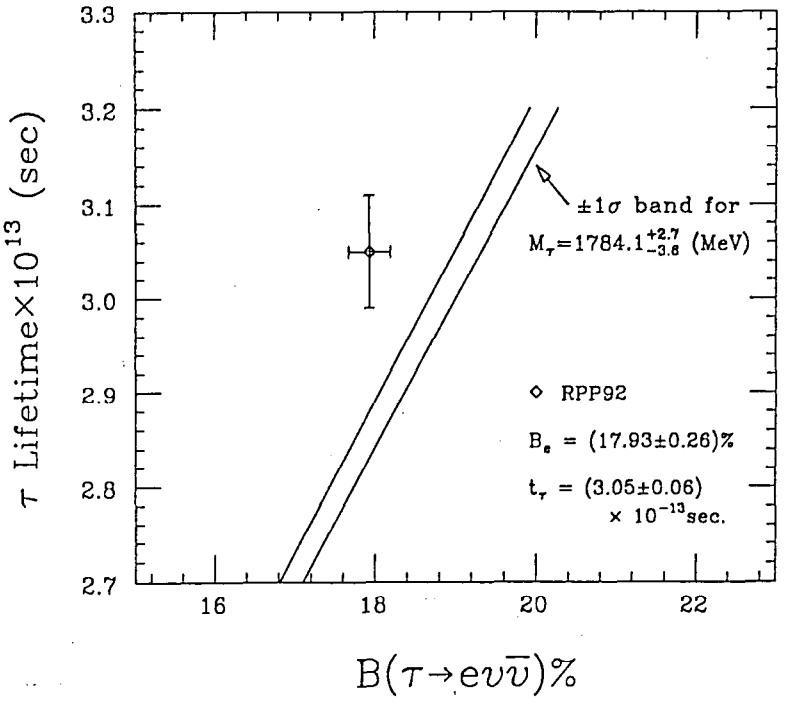

Figure 2: The variation of t_τ with B_τ^e given by Equation (6) under the assumption of lepton universality; the $\pm 1\sigma$ band is obtained using the RPP92 value of the tau mass $m_\tau = 1784.1^{+2.7}_{-3.6}$ MeV. The point with error bars is derived from the RPP92 values for the tau electronic branching fraction and tau lifetime.

final state, with one τ decaying via $e\nu\bar{\nu}$ and the other via $\mu\nu\bar{\nu}$. In addition, BES chooses to measure the threshold behavior of the cross section in the narrow range of center-of-mass energy, $3.544 \leq W \leq 3.569$ GeV, according to a scan strategy to be described later. This procedure results in a measurement of the tau mass to a few *tenths* MeV uncertainty.

2 The Beijing Collider and the Beijing Spectrometer

The Beijing Electron Positron Collider[5],shown in Figure 6, operates in the 3 to 5 GeV center-of-mass energy range. Near $\tau^+\tau^-$ threshold,the peak luminosity is 5×10^{30} cm^{-2}s^{-1}, the luminosity-weighted uncertainty in the mean center-of-mass energy is 0.10 MeV, and the spread in the center-of-mass energy of the collider is $\approx$ 1.4 MeV. The absolute energy scale and energy spread are determined by interpolation between the results of repeated scans of the J/ψ and $\psi(2S)$ resonances.

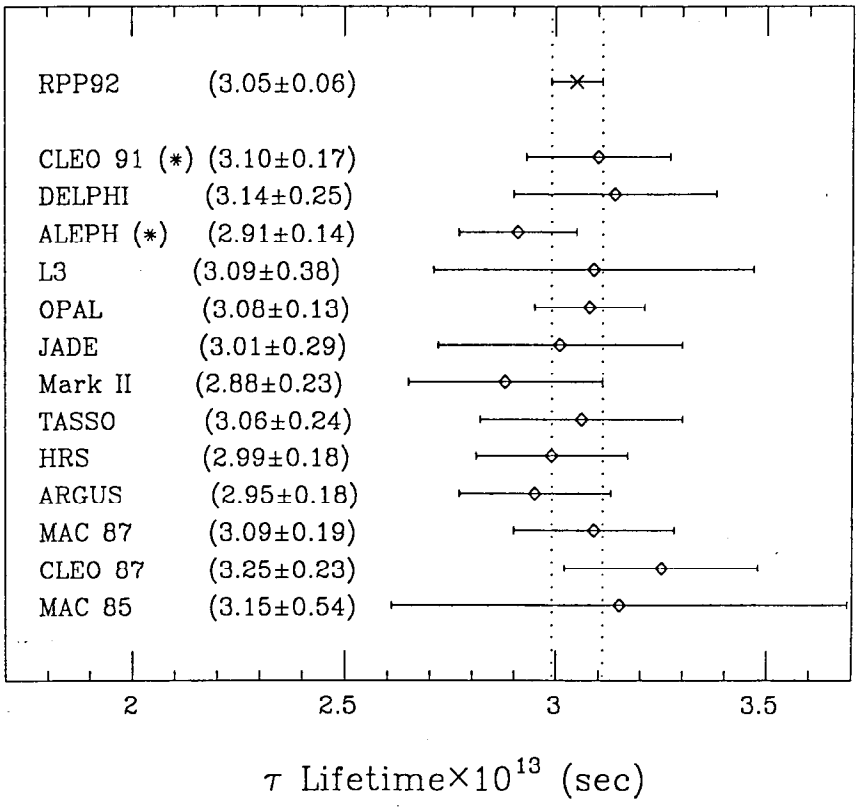

Figure 3: Tau lifetime measurements as listed in RPP92 (some of the older values have actually been dropped from the average).

The Beijing Spectrometer[5], shown in Figure 7, is a solenoidal detector with a 0.4 T magnetic field. Charged track reconstruction is performed by means of a cylindrical drift chamber which provides solid angle coverage of 85% of 4π. The momentum resolution is $\sigma_p/p = 0.021\sqrt{1+p^2}$ (p in GeV/c). Measurements of dE/dx with resolution 8.5% allow particle identification. An inner drift chamber is used for trigger purposes. Scintillation counters measure the time-of-flight of charged particles over 76% of 4π with a Bhabha resolution of 330 ps. A cylindrical twelve-radiation-length Pb/gas electromagnetic calorimeter operating in limited streamer mode covering 80% of 4π achieves energy resolution $\sigma_E/E = 0.25/\sqrt{E(\mathrm{GeV})}$, and spatial resolution $\sigma_\phi = 4.5$ mrad, $\sigma_z = 2$ cm. End-cap time-of-flight counters and shower counters are not used in this analysis. Finally, a three-layer iron flux return instrumented for muon identification yields spatial resolutions $\sigma_z = 5$ cm, $\sigma_{r\phi} = 3$ cm over 68% of 4π for muons with momentum greater than 550 MeV/c.

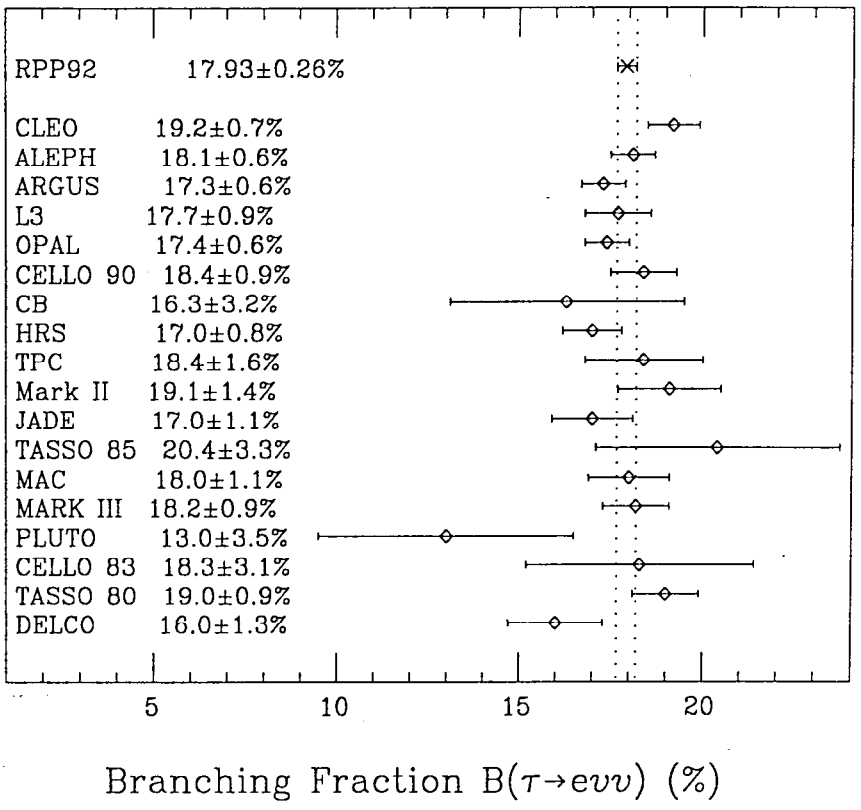

Figure 4: Tau electronic branching fraction measurements as listed in RPP92.

3 Event Selection

In the data analysis, the event selection for $e\mu$ candidates requires : (1) exactly two oppositely-charged tracks having momentum between 350 MeV/c and the maximum for an electron from τ decay; (2) each track's point of closest approach to the beam axis to satisfy $|x| < 1.5$ cm, $|y| < 1.5$ cm and $|z| < 15$ cm; (3) $2.5° < \theta_{\rm acol} < 177.5°$, $\theta_{\rm acop} > 10°$(see Reference [6]), and $(\theta_{\rm acol} + \theta_{\rm acop}) > 50°$; (4) no isolated photons;[†] (5) one track well-identified as a muon in the muon-counter, with calorimeter energy < 500 MeV, and the other track well-identified as an electron using a combination of calorimeter, dE/dx and time-of-flight information. A typical candidate event is shown in Figure 8. Monte Carlo simulations yield a detection efficiency of $\approx 14\%$ for these selection criteria. The background is estimated by applying the same requirements to five million events from a data sample taken at the J/ψ energy; seven events meet these criteria, corresponding to a background of 0.12 events in the entire $\tau^+\tau^-$ sample.

[†]An isolated photon has an energy > 60 MeV and is separated from the nearest charged track by $> 12°$.

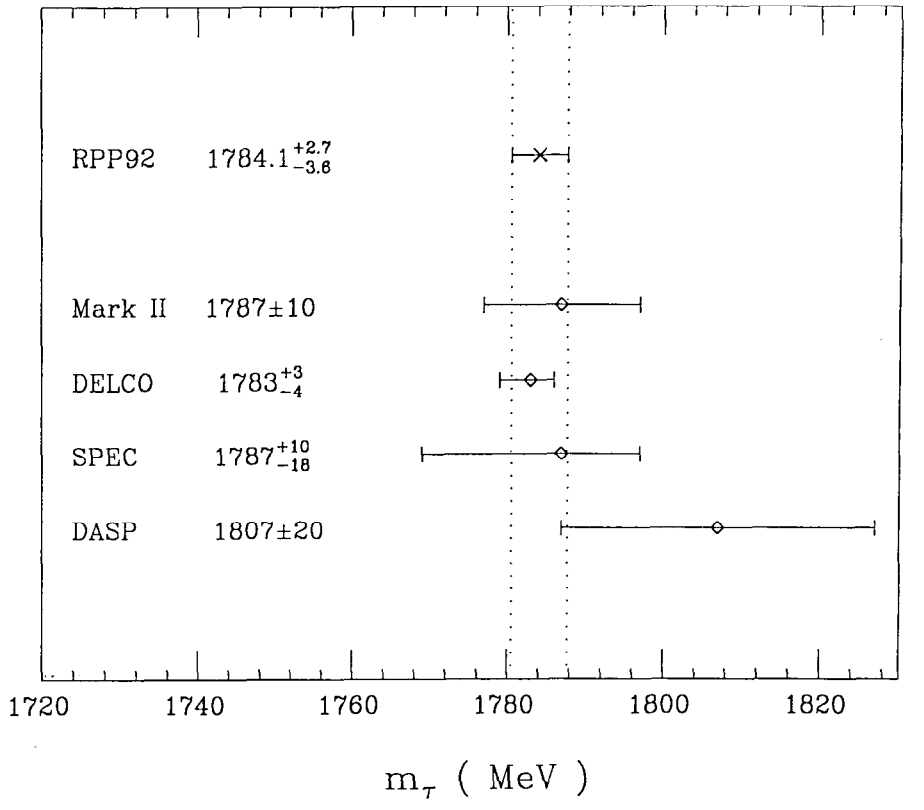

Figure 5: Tau mass measurements as listed in RPP92.

4 $\tau^+\tau^-$ Production Cross Section Near Threshold

The likelihood function used to estimate the τ mass incorporates the $\tau^+\tau^-$ cross section near threshold. Including the center-of-mass energy spread Δ, initial state radiation[7] $F(x, W)$, and vacuum polarization corrections[8] $\Pi(W)$, the cross section is

$$\sigma(W, m_\tau) = \frac{1}{\sqrt{2\pi}\Delta} \int_0^\infty dW' e^{\frac{-(W-W')^2}{2\Delta^2}} \int_0^{1-\frac{4m_\tau^2}{W'^2}} dx F(x, W') \sigma_1(W'\sqrt{1-x}, m_\tau), \quad (9)$$

where σ_1 is given by

$$\sigma_1(W, m_\tau) = \frac{4\pi\alpha^2}{3W^2} \frac{\beta(3-\beta^2)}{2} \frac{F_c(\beta) F_r(\beta)}{[1-\Pi(W)]^2}, \quad (10)$$

W is the center-of-mass energy, and $\beta = \sqrt{1-(\frac{2m_\tau}{W})^2}$. The Coulomb interaction and final state radiation corrections are described[9] by the functions $F_c(\beta)$

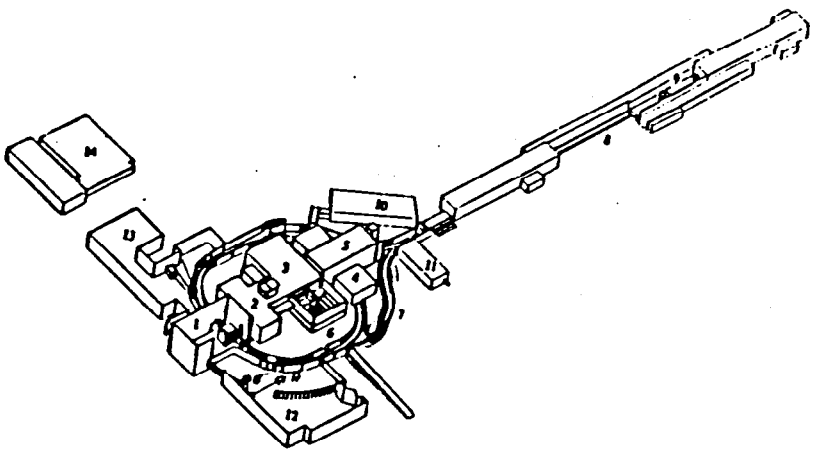

Figure 6: The Beijing Electron Positron Collider (BEPC). At the right of the figure is shown the 202 meter injection linac leading to the 240 meter circumference storage ring in the lower left. The electrons circulate in the clockwise direction and the positrons circulate counter-clockwise. The BES detector sits on the side of the ring opposite the injection linac.

and $F_\tau(\beta)$. The effect of these different corrections on the lowest order QED cross section is shown in Figure 9. The cross section was coded independently at Caltech and IHEP Beijing and the two efforts were found to be in agreement.

5 Strategy of the Center-of-Mass Energy Scan

For an observed set of events

$$\vec{N} = (N_1, N_2, N_3, ..., N_n), \tag{11}$$

at center of mass energies

$$\vec{W} = (W_1, W_2, W_3, ..., W_n), \tag{12}$$

a likelihood function is formed according to

$$\mathcal{L}(\vec{N}, m_\tau) = \prod_{i=1}^{n} \frac{\mu_i^{N_i} e^{-\mu_i}}{N_i!}, \tag{13}$$

with the expected number of observed $e\mu$ events at center-of-mass energy W_i given by

$$\mu_i = [\epsilon\ B\ \sigma(W_i, m_\tau) + \sigma_b] \times L_i\ , \tag{14}$$

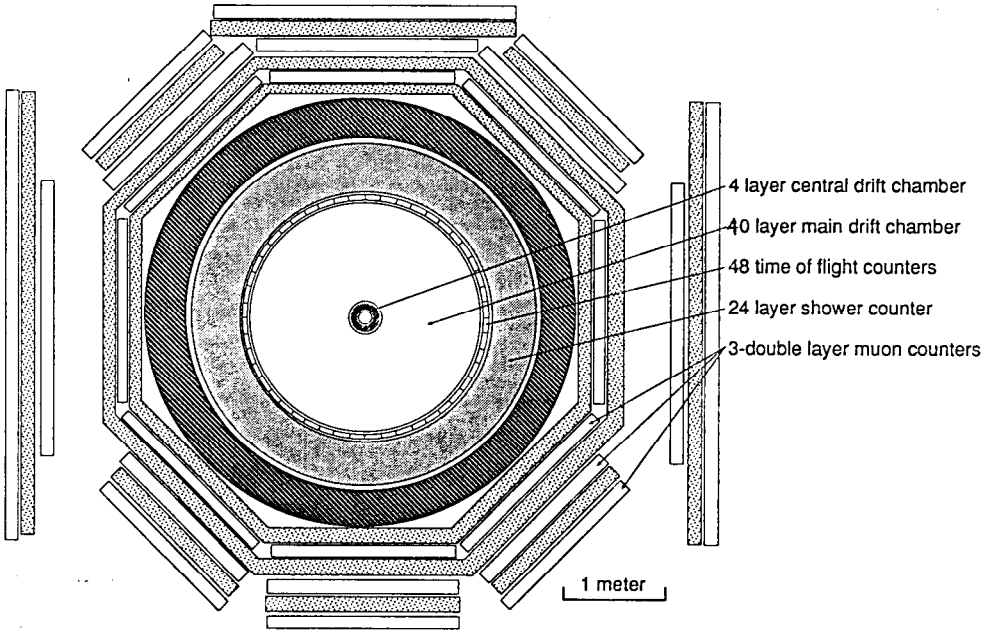

Figure 7: The Beijing Spectrometer (BES).

where ϵ = detection efficiency, $B = 2B_\tau^e B_\tau^\mu$, L = integrated luminosity at scan point i, and σ_b is the effective background cross section estimated from the J/ψ data sample ($\sigma_b = 0.024$pb). The best estimate of the value of m_τ is obtained by maximizing the likelihood function $\mathcal{L}$ with respect to m_τ.

Since the range of center-of-mass energies where the $\tau^+\tau^-$cross section is most sensitive to the τ mass is of the order of the beam energy spread around $\tau^+\tau^-$ threshold, it is important to devise a running strategy to maximize the integrated luminosity in this region. The beam energy is set initially assuming the world average for the τ mass, in this case the RPP92 value 1784.1 MeV. Then, after each 250 – 400 nb^{-1} of integrated luminosity, a new estimate of the mass is made using all the data accumulated to that point; in this way a new prediction of the most sensitive energy at which to run is obtained. The energy is changed to this new value if the difference is more than the BEPC step size ($\approx$ 0.4 MeV). Following this strategy, an integrated luminosity of $\approx$ 4.3 pb^{-1} has been accumulated at ten energies within a range of 24 MeV. It has been verified by Monte Carlo simulation that this data-driven search strategy provides an unbiased measurement of the tau mass.

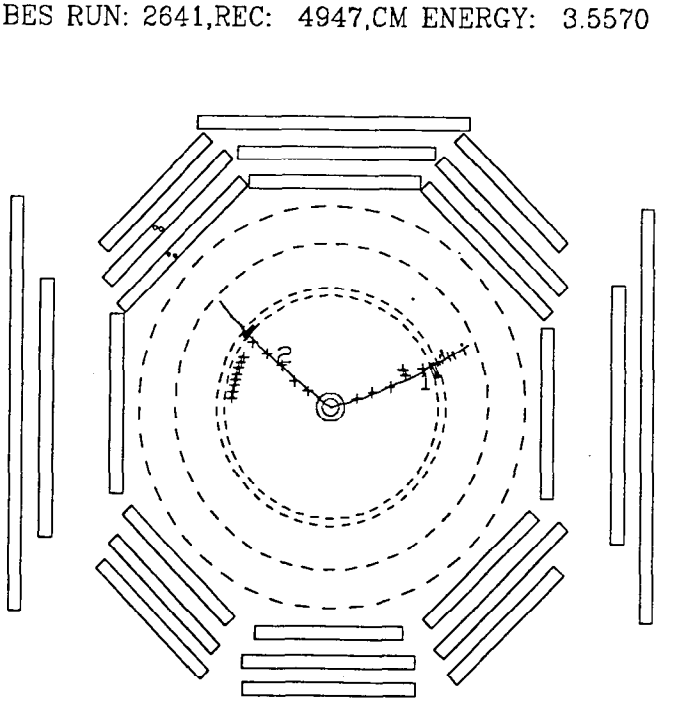

Figure 8: A typical $e\mu$ event candidate. Notice that track 1 ends in a shower in the electromagnetic calorimeter and that track 2 penetrates two layers of the muon system.

The sequence of energies is shown in Figure 10 and the corresponding data[10] are summarized in Table 2. The ten-step search yielded seven $e\mu$ events. The eleventh and twelfth points in Table 2, taken well above threshold where the cross section is a slowly varying function of the center-of-mass energy, provide an improved estimate of the absolute $\tau^+\tau^-$ cross section.

6 Result of the Maximum Likelihood Fit

In order to account for uncertainties in the efficiency ϵ, the branching fraction product and the luminosity, ϵ is treated as a free parameter in a two-dimensional maximum-likelihood fit for m_τ and ϵ to the data of Table 2. The likelihood function corresponding to the fit is shown in Figure 11, and the estimates obtained are $m_\tau = 1776.9$ MeV and $\epsilon = 14.1$ %. The uncertainty in ϵ is equivalent to the uncertainty in the absolute normalization, and is treated as a source of systematic error. The statistical error[11] in m_τ, $^{+0.4}_{-0.5}$ MeV, is determined from the one-parameter likelihood function with ϵ fixed to 14.1% (Figure 12). The

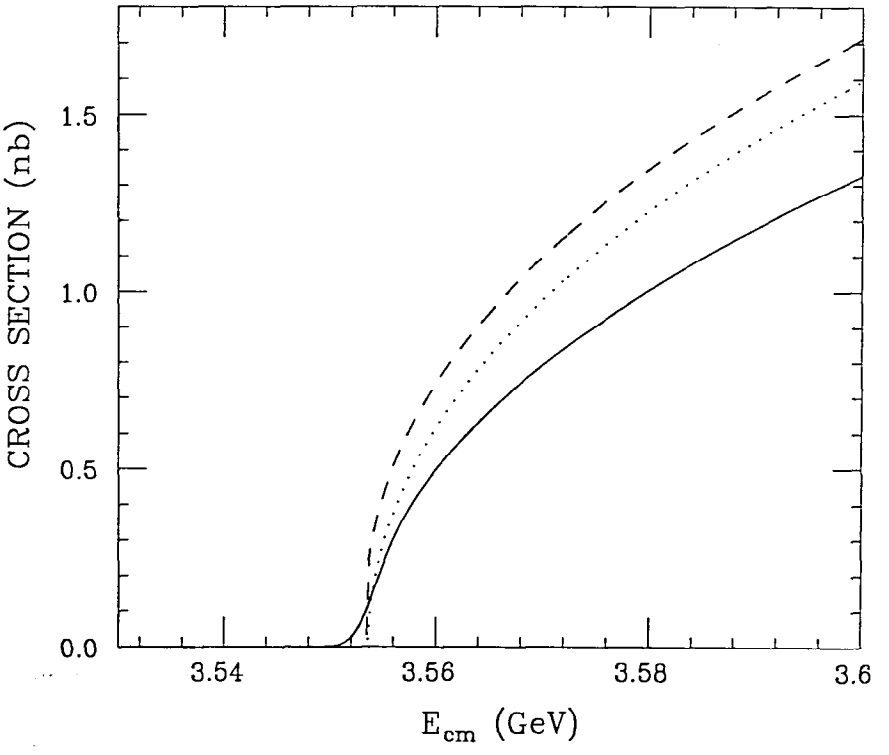

Figure 9: The $\tau^+\tau^-$ production cross section near threshold. The dotted line shows the lowest order QED cross section, the dashed line takes into account the Coulomb interaction and final state radiation and the solid line shows the final cross section used in this analysis after initial state radiation, vacuum polarization and beam energy spread have been taken into account. Note that the beam energy spread smears out the sharp step at threshold caused by the Coulomb interaction.

efficiency-corrected cross section data as a function of corrected beam energy, and the curve which results from the likelihood fit, are shown in Figure 12. The quality of the fit is checked by forming the likelihood ratio λ with result[12] $-2\ln\lambda = 3.6$.

7 Systematic Errors

Four independent sources of systematic error are considered: uncertainties in the product $\epsilon B\mathcal{L}$, in the absolute beam energy scale, in the beam energy spread, and in the background.

The systematic uncertainty in $\epsilon B\mathcal{L}$ is determined by fixing m_τ at its best estimate value and finding the values of ϵ corresponding to $\pm 1\sigma$ variations

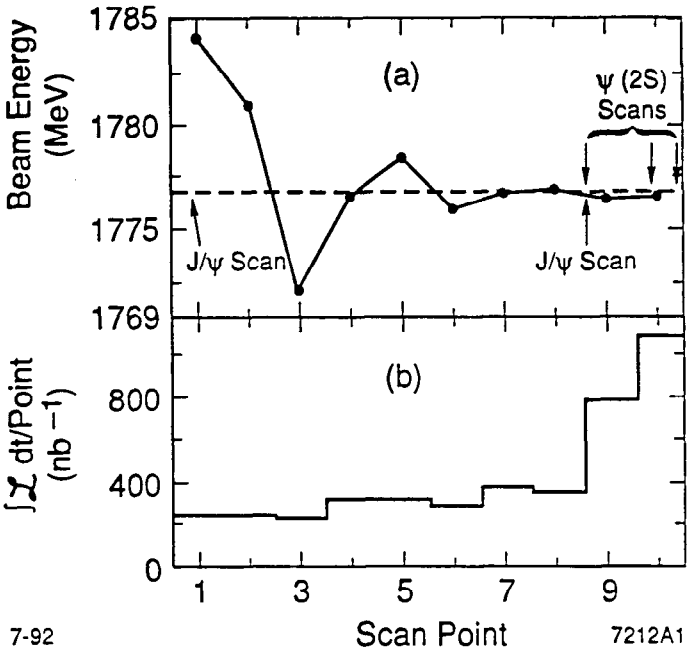

Figure 10: (a) The convergence of the predicted mass with each consecutive scan point. (b) The integrated luminosity accumulated at each point. Note that the luminosity per scan point is approximately constant for the first 8 points. For the last two points it increases significantly; this is because the likelihood fit indicates that no change in beam energy is required as the correct threshold is approached.

in the likelihood function; these efficiencies are 18.3% and 10.6%. Fixing the efficiency to each of these values in turn and fitting for m_τ yields changes in the predicted mass of $\Delta m_\tau = {}^{+0.16}_{-0.20}$ MeV.

The energy scale is determined from several scans of the J/ψ and $\psi(2S)$ shown in Figure 13 performed during the search (see Figure 10). From the data in Figure 13(a) the values $\bar{M}_\psi = 3097.20$ MeV and $\delta M_\psi = |3097.32 - 3097.07|/\sqrt{2} = 0.18$ MeV are obtained, and from the data in Figure 13(b) $\bar{M}_{\psi'} = 3686.88$ MeV and $\delta M_{\psi'} = \sqrt{(0.15)^2 + 0.0^2 + (0.14)^2}/\sqrt{2} = 0.15$ MeV. The reproducibility of the fits to these scans, together with the other uncertainties listed in Table 3, yields[13] a systematic uncertainty of $\Delta m_\tau = \pm 0.09$ MeV.

Fits to the two resonances were also used to measure the beam energy spread and its variation with center-of-mass energy and beam current. The uncertainty in center-of-mass energy spread is ± 0.08 MeV, yielding a systematic error $\Delta m_\tau = \pm 0.02$ MeV.

Table 2: A chronological summary of the $\tau^+\tau^-$ data.

Scan Point	$W/2$ (MeV)	Δ (MeV)	$\mathcal{L}$ (nb^{-1})	N ($e\mu$ events)
1	1784.19	1.34	245.8	2
2	1780.99	1.33	248.9	1
3	1772.09	1.36	232.8	0
4	1776.57	1.37	323.0	0
5	1778.49	1.44	322.5	2
6	1775.95	1.43	296.9	0
7	1776.75	1.47	384.0	0
8	1776.98	1.47	360.8	1
9	1776.45	1.44	794.1	0
10	1776.62	1.40	1109.1	1
11	1799.51	1.44	499.7	5
12	1789.55	1.43	250.0	2

Finally, the systematic error due to uncertainty in the background is estimated from the 1σ Poisson errors on the seven J/ψ background events and the uncertainty in the hadronic cross section at $\tau^+\tau^-$ threshold. The resulting uncertainty is $\Delta m_\tau = \pm 0.01$ MeV.

These independent systematic errors are added in quadrature to yield a total systematic error of $\Delta m_\tau = {}^{+0.18}_{-0.22}$ MeV.

Table 3: Contributions to the uncertainty in the energy scale.

Quantity	Error (MeV)
W_M : BEPC measured center-of-mass energy	$\delta W_M = 0.10$
M_ψ : BEPC value for J/ψ mass	$\delta M_\psi = 0.18$
$M_{\psi'}$: BEPC value for $\psi(2S)$ mass	$\delta M_{\psi'} = 0.15$
T_ψ : RPP92 value for J/ψ mass[2]	$\delta T_\psi = 0.09$
$T_{\psi'}$: RPP92 value for $\psi(2S)$ mass[2]	$\delta T_{\psi'} = 0.10$

8 CONCLUSION

In conclusion, using a maximum likelihood fit to $\tau^+\tau^-$ cross section data near threshold, the mass of the τ lepton has been measured as $m_\tau = 1776.9^{+0.4}_{-0.5} \pm 0.2$ MeV, where the first error is statistical and the second systematic. This result is 7.2 MeV below the RPP92 average[2] as shown in Figure 14, and has significantly smaller errors.[14] Inserting this new value in Equation (6), the coupling strength ratio becomes

$$\left(\frac{G_{\tau\to e\nu\bar{\nu}}}{G_{\mu\to e\nu\bar{\nu}}}\right)^2 = 0.960 \pm 0.024, \tag{15}$$

so that the deviation from lepton universality is reduced from 2.4 to 1.7 standard deviations (see Figure 15; see also Reference [15] for an updated value of this ratio which takes into account more recent tau lifetime and electronic branching fraction measurements). It should be noted also that this new result for m_τ yields a reduction in the upper limit on m_{ν_τ}.

9 ACKNOWLEDGEMENTS

The author would like to thank the many colleagues who helped in the preparation of this talk and in particular Bill Dunwoodie for a critical reading of the manuscript.

The BES Collaboration would like to thank the BEPC staff and the Computer Center at IHEP for their outstanding efforts and also Y. S. Tsai and J. M. Wu for helpful discussions about the $\tau^+\tau^-$ cross section near threshold. This work was supported in part by the National Natural Science Foundation of China under Contract No. 19290400, by the U. S. Department of Energy under Contracts No. DE-FG03-92ER40701, No. DE-FG03-91ER40679, No. DE-FG02-91ER40676, No. DE-AC02-76ER03069, No. DE-AC35-89ER40486, No. DE-AC03-76SF00515, and No. DE-FG05-92ER40736, by the Texas National Research Laboratory Commission (Rocky Mountain Consortium for High Energy Physics) under Contracts No. RGFY91B5 and No. RGFY92B5, and by the National Science Foundation.

References

The BES Collaboration

[1] J. Z. Bai[a] O. Bardon[g] R. A. Becker-Szendy[h] A. Breakstone[f] T. H. Burnett[k] J. S. Campbell[j] S. J. Chen[a] S. M. Chen[a]

Y. Q. Chen[a] Z. D. Cheng[a] J. A. Coller[b] R. F. Cowan[g] H. C. Cui[a] X. Z. Cui[a] H. L. Ding[a] Z. Z. Du[a] W. Dunwoodie[h] C. Fang[a] M. J. Fero[g] M. L. Gao[a] S. Q. Gao[a] W. X. Gao[a] Y. N. Gao[a] J. H. Gu[a] S. D. Gu[a] W. X. Gu[a] Y. N. Guo[a] Y. Y. Guo[a] Y. Han[a] M. Hatanaka[c] J. He[a] D. G. Hitlin[c] G. Y. Hu[a] T. Hu[a] D. Q. Huang[a] Y. Z. Huang[a] J. M. Izen[j] Q. P. Jia[a] C. H. Jiang[a] Z. J. Jiang[a] A. S. Johnson[b] L. A. Jones[c] M. H. Kelsey[c] Y. F. Lai[a] P. F. Lang[a] A. Lankford[d] F. Li[a] J. Li[a] P. Q. Li[a] Q. M. Li[a] R. B. Li[a] W. Li[a] W. D. Li[a] W. G. Li[a] Y. S. Li[a] S. Z. Lin[a] H. M. Liu[a] Q. Liu[a] R. G. Liu[a] Y. Liu[a] B. Lowery[j] J. G. Lu[a] D. H. Ma[a] E. C. Ma[a] J. M. Ma[a] M. Mandelkern[d] H. Marsiske[h] H. S. Mao[a] Z. P. Mao[a] X. C. Meng[a] H. L. Ni[a] S. L. Olsen[f] L. J. Pan[a] J. H. Panetta[c] F. C. Porter[c] E. N. Prabhakar[c] N. D. Qi[a] Y. K. Que[a] J. Quigley[g] G. Rong[a] B. Schmid[d] J. Schultz[d] J. T. Shank[b] Y. Y. Shao[a] D. L. Shen[a] H. Y. Sheng[a] H. Z. Shi[a] A. Smith[d] E. Soderstrom[h] X. F. Song[a] D. P. Stoker[d] H. S. Sun[a] J. Synodinos[h] W. H. Toki[e] G. L. Tong[a] E. Torrence[g] L. Z. Wang[a] M. Wang[a] P. Wang[a] P. L. Wang[a] T. J. Wang[a] Y. Y. Wang[a] J. S. Whitaker[b] R. J. Wilson[b] W. J. Wisniewski[i] X. D. Wu[a] D. M. Xi[a] X. M. Xia[a] P. P. Xie[a] X. X. Xie[a] R. S. Xu[a] Z. Q. Xu[a] S. T. Xue[a] R. K. Yamamoto[g] J. Yan[a] W. G. Yan[a] C. M. Yang[a] C. Y. Yang[a] H. B. Yao[a] M. H. Ye[a] S. Z. Ye[a] Z. Q. Yu[a] B. Y. Zhang[a] C. C. Zhang[a] D. H. Zhang[a] H. L. Zhang[a] H. Y. Zhang[a] J. W. Zhang[a] L. S. Zhang[a] S. Q. Zhang[a] Y. Zhang[a] D. X. Zhao[a] M. Zhao[a] P. D. Zhao[a] W. R. Zhao[a] J. P. Zheng[a] L. S. Zheng[a] Z. P. Zheng[a] G. P. Zhou[a] H. S. Zhou[a] L. Zhou[a] L. Zhou[a] X. F. Zhou[a] Y. H. Zhou[a] Q. M. Zhu[a] Y. C. Zhu[a] Y. S. Zhu[a] G. Zioulas[d]

[a] Institute of High Energy Physics, Beijing 100039, People's Republic of China.

[b] Boston University, Boston MA 02215, U.S.A.

[c] California Institute of Technology, Pasadena CA 91125, U.S.A.

[d] University of California, Irvine CA 92717, U.S.A.

[e] Colorado State University, Fort Collins CO 80523, U.S.A.

[f] University of Hawaii, Honolulu, HI 96822 U.S.A.

[g] Massachusetts Institute of Technology, Cambridge MA 02139, U.S.A.

[h] Stanford Linear Accelerator Center, Stanford CA 94309, U.S.A.

[i] Superconducting Super Collider Laboratory, Dallas TX 75237-3946, U.S.A.

[j] University of Texas at Dallas, Richardson TX 75083-0688, U.S.A.

[k] University of Washington, Seattle WA 98195, U.S.A.

[2] K. Hikasa *et al.* Review of Particle Properties, *Phys. Rev.* **D45**, Part II (1992)

[3] W. J. Marciano and A. Sirlin, *Phys. Rev. Lett.* **61** (88) 1815.

[4] W. Bacino *et. al.*, *Phys. Rev. Lett.* **41**, (78) 13.
see also J. Kirz in the 1978 Tokyo Conference proceedings, page 249.

[5] M. H. Ye and Z. P. Zheng, in *Proceedings of the 1989 International Symposium on Lepton and Photon Interactions at High Energies* (Stanford University, Stanford, 1989) page 122.

[6] Acoplanarity, $\theta_{\rm acop}$, is defined as the angle between the planes spanned by the beam direction and the momentum vector of the e and μ respectively. Acollinearity, $\theta_{\rm acol}$, is defined as the angle between the momentum vectors of the e and μ.

[7] É. A. Kuraev and V. S. Fadin, *Yad. Fiz.* **41** (85) 733.

[8] F. A. Berends and G. J. Komen, *Phys. Lett.* **63B** (76) 432.

[9] M. B. Voloshin, TPI-MINN-89-33-T, Nov. 1989.

[10] The center-of-mass energy spread Δ was determined according to the equation $\Delta = (A\bar{I}+B)(CW^2+D)$, where $\bar{I}$ is the average beam current. A, B, C and D are fitted to beam current measurements and to measurements of the energy spreads at the J/ψ and $\psi(2S)$ resonances.

[11] It has been verified by simulation that this uncertainty corresponds to a 68% confidence interval.

[12] In the large statistics limit, $-2\ln\lambda$ would obey a χ^2 distribution for ten degrees of freedom.

[13] Assuming a linear relation between measured energy W_M, and the corrected value W, the latter is given by :

$$W = T_\psi + (W_M - M_\psi)\Big(\frac{T_{\psi'} - T_\psi}{M_{\psi'} - M_\psi}\Big)$$

in the notation of Table 3. At $\tau^+\tau^-$ threshold the resulting mass scale correction is $W - W_M = -0.74$ MeV, with corresponding uncertainty $\delta W = 0.18$ MeV.

[14] The Argus Collaboration has also reported (H. Albrecht *et al.*, *Phys. Lett.* 292**B** (92) 221. a new measurement of the τ mass, $m_\tau = 1776.3 \pm 2.4 \pm 1.4$ MeV; the CLEO II Collaboration have reported at this conference a further new measurement $m_\tau = 1777.6 \pm 0.9 \pm 1.5$ MeV

[15] H. Marsiske, SLAC-PUB-5977, Nov. 1992.

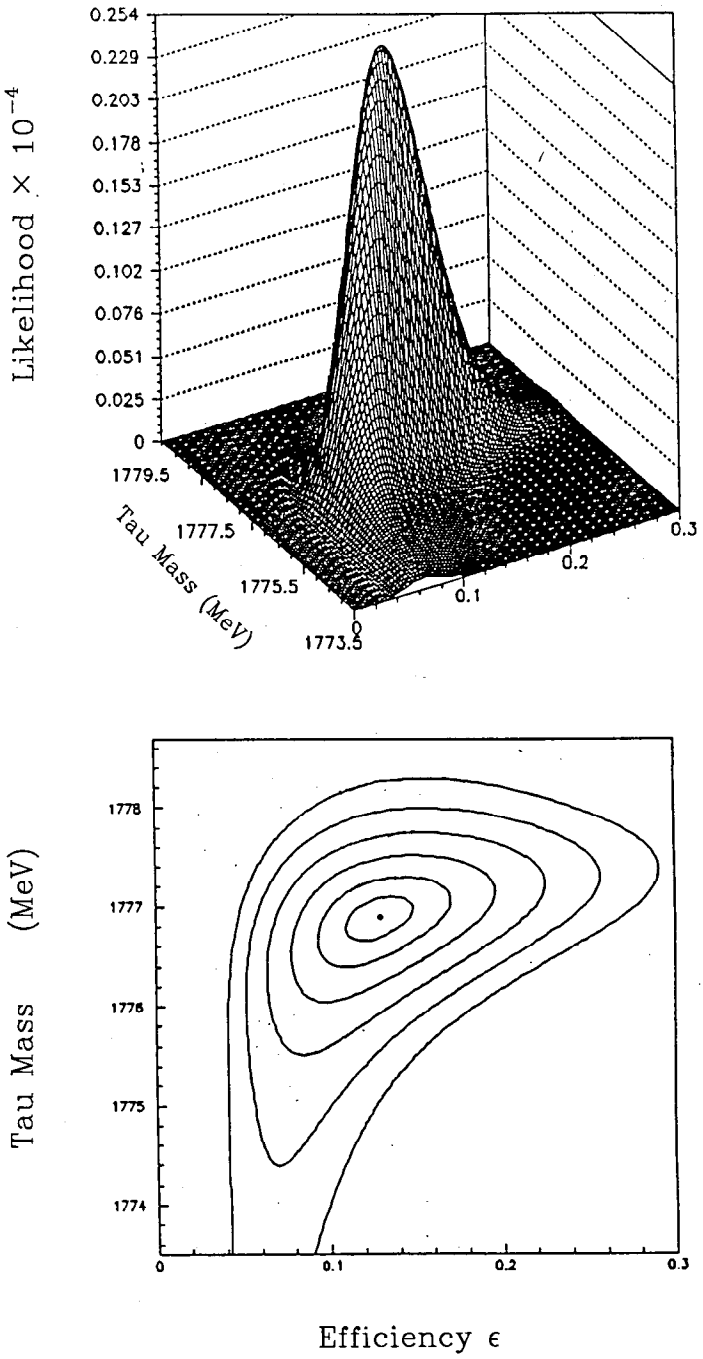

Figure 11: (a) the two dimensional likelihood function for the data in Table 2; (b) the projection of (a) showing 1/2 σ contours.

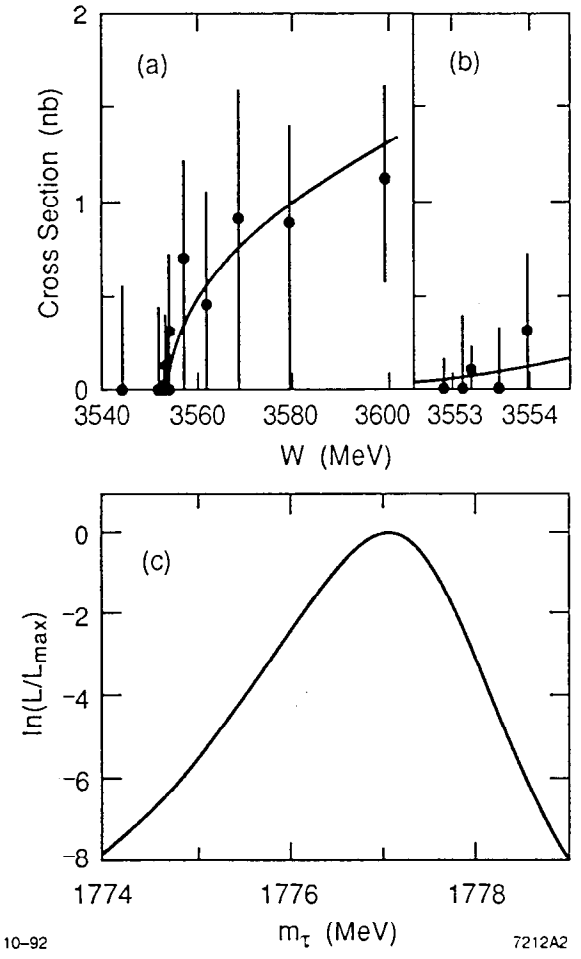

Figure 12: (a) The center-of-mass energy dependence of the $\tau^+\tau^-$ cross section resulting from the likelihood fit (curve), compared to the efficiency-corrected data. The error bar on each data point is computed by integrating the Poisson likelihood function to obtain the interval containing 68% of the area. It should be emphasized that the curve does not result from a direct fit to these data points. (b) An expanded version of (a), in the immediate vicinity of $\tau^+\tau^-$ threshold. (c) The dependence of the logarithm of the likelihood function on m_τ, with efficiency fixed at 14.1%.

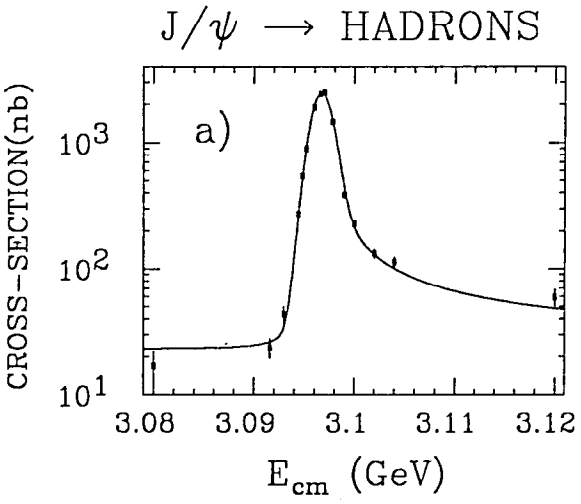

Scans During Tau Data Taking

Mass (MeV)	Δ (MeV)
3097.32±0.02	1.04±0.017
3097.07±0.02	1.20±0.016

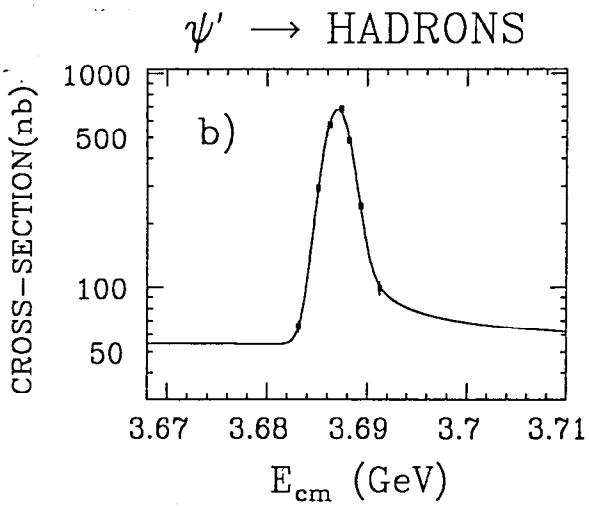

Mass (MeV)	Δ (MeV)
3687.03±0.03	1.49±0.043
3686.88±0.03	1.34±0.038
3686.74±0.03	1.40±0.024

Figure 13: (a) the J/ψ and (b) $\psi(2S)$ fit parameters used to determine the energy scale.

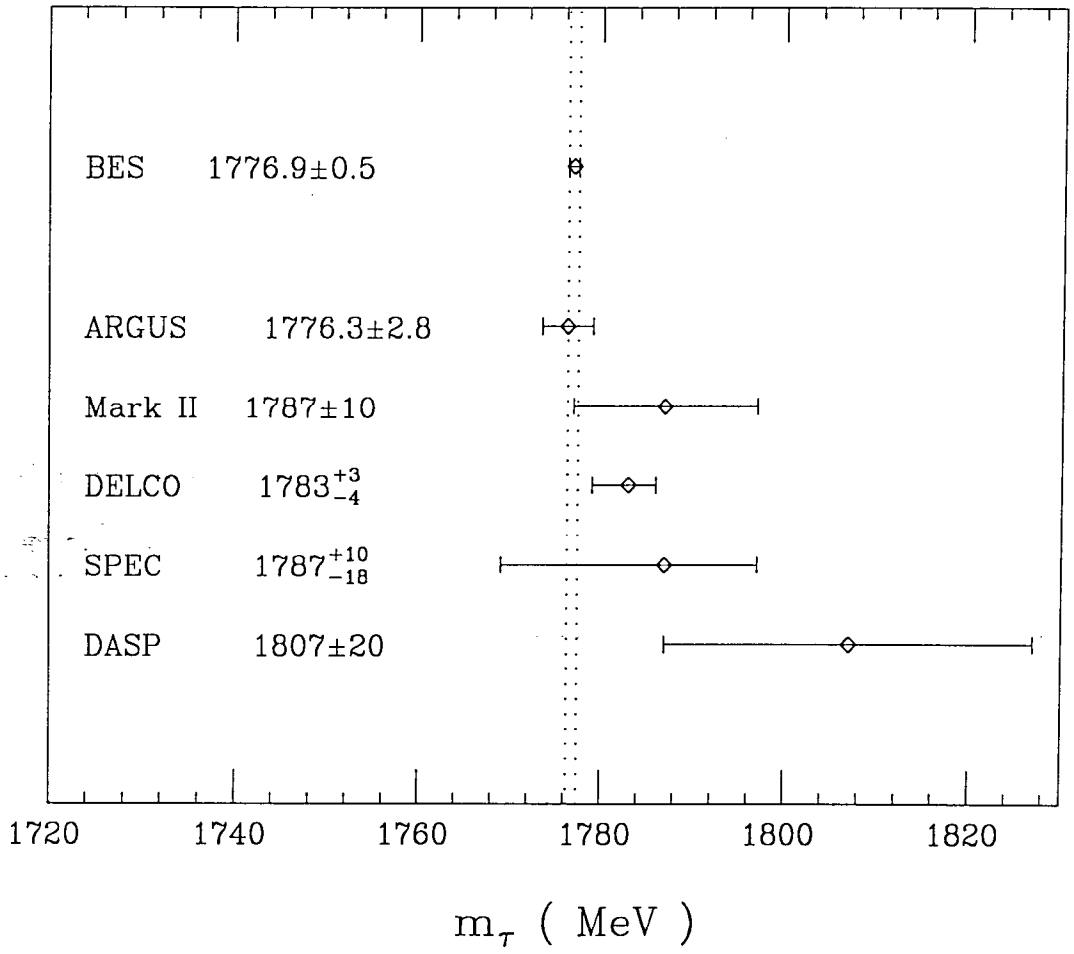

Figure 14: Tau Mass Measurements.

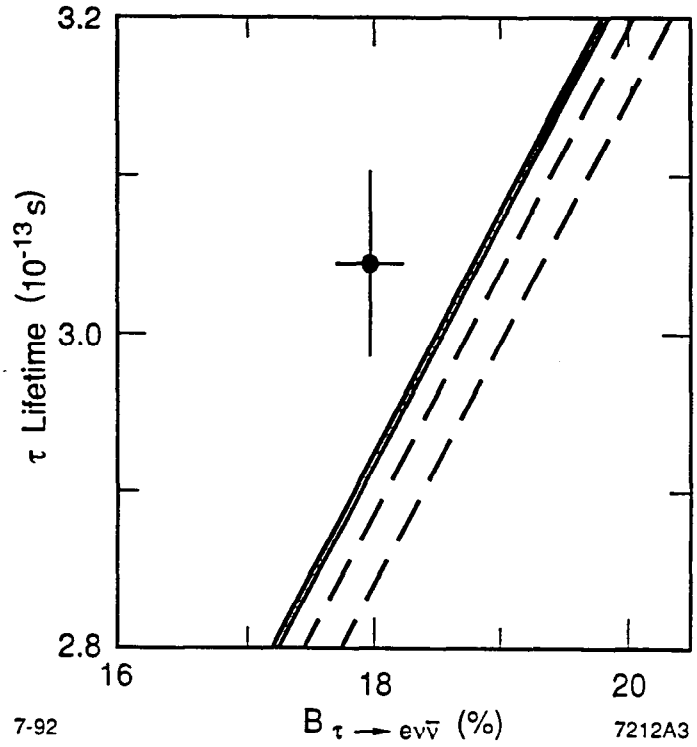

Figure 15: The variation of t_τ with B_τ^e, given by Equation (6) under the assumption of lepton universality; the $\pm 1\sigma$ bands obtained using m_τ from this experiment (solid lines) and using the RPP92 value (dashed lines) are shown in comparison to the point corresponding to the RPP92 values (1σ error bars).